Supporting Information

Helical Nanoplatelet Superlattices Assembled from Green Emissive $CsPbI_3$ Nanoplatelets

Author Name: Liguo Zhang[a,#], Qiangsheng Chen[a,#], Baowei Zhang[a,], Siyu Lu[a,*]*

Author Address: [a]College of Chemistry, Pingyuan Laboratory, Zhengzhou University, Zhengzhou, 450000, China.

AUTHOR INFORMATION

Corresponding Author

*Email: baoweizhang@zzu.edu.cn; sylu2013@zzu.edu.cn.

Experimental Section

Materials

Lead iodide (PbI_2, 99%), Cesium carbonate (Cs_2CO_3, 99%), Zinc iodide (ZnI_2, 99%), Oleylamine (OAm, 70%), Erucic acid (85%), (R)-(+)-methylbenzylamine (R-MBA, 99%), (S)-(-)-methylbenzylamine (S-MBA, 99%), Octane (99%), Heptane (99%), 1-Octadecene (70%) and Oleic acid (OA, 70%) were purchased from Sigma-Aldrich. Oleylamine (70%), Oleic acid (70%) and 1-Octadecene (70%) were degassed and stored in the glovebox before use. Toluene was purchased from General Reagents (they were degassed to remove residual water before use). All the other chemicals were used without any further purifications.

Methods

Preparation of Cesium oleate: 0.4 g (1.23 mmol) of Cs_2CO_3 and 16 mL of OA was added into a 50 mL three-neck flask. This mixture was heated at 80 °C for 1 hour under vacuum. The Cs_2CO_3 was dissolved and became transparent, colorless solution. Subsequently, the mixture was cooled down to room temperature under nitrogen atmosphere, and then was transferred to a 20 mL glass vial for later use.

Synthesis of $CsPbI_3$ NCs: PbI_2 (96 mg, 0.21 mmol), ZnI_2 (67 mg, 0.21 mmol), 0.75 mL oleic acid, 0.75 mL oleylamine, and 5 mL ODE were mixed together into a 25 mL three-neck flask[1]. This mixture was heated at 120 °C for 1 hour under vacuum to dissolve the metal precursors. Afterward, the temperature was raised to 170 °C, followed by a rapid injection of 0.5 mL cesium oleate solution. After 15 seconds, the flask was immediately immersed in an ice-water bath to quench the reaction. The solution was centrifuged at 6000 rpm for 10

minutes, the supernatant was decanted, and the centrifuged solid was dispersed in toluene for further characterizations.

Synthesis of $CsPbI_3$ NPLs (n=1): PbI_2 (96 mg, 0.21 mmol), ZnI_2 (0.12 g, 0.38 mmol), 0.62 mL erucic acid, 0.75 mL oleylamine, and 5 mL ODE were mixed together into a 25 mL three-neck flask. This mixture was heated at 120 °C for 60 minutes under vacuum to dissolve the metal precursors. Afterward, the temperature was set up as 80 °C, followed by a rapid injection of 0.5 mL cesium oleate solution. After 5 seconds, the flask was immediately immersed in a water bath to quench the reaction. The solution was centrifuged at 3500 rpm for 7 minutes, the supernatant was decanted, and the centrifuged solid was dispersed in toluene for further characterizations and assembly experiments.

Synthesis of $CsPbI_3$ NPLs (n=2): PbI_2 (96 mg, 0.21 mmol), ZnI_2 (67 mg, 0.21 mmol), 0.62 mL erucic acid, 0.75 mL oleylamine, and 5 mL ODE were mixed together into a 50 mL three-neck flask. This mixture was heated at 120 °C for 45 minutes under nitrogen to dissolve the metal precursors. Afterward, the temperature was set up as 80 °C, followed by a rapid injection of 0.5 mL cesium oleate solution. After 5 seconds, the flask was immediately immersed in a water bath to quench the reaction. The solution was centrifuged at 3500 rpm for 7 minutes, the supernatant was decanted, and the centrifuged solid was dispersed in toluene for further characterizations and assembly experiments.

Synthesis of R/S-MBA carbon dots: Transfer 10 mL of R/S-MBA solution into a Teflon-lined autoclave (25 mL), and heat it at 200°C for 12 hours. Then, let it cool to room temperature.

Ligand exchange with R/S-MBA or R/S-MBA carbon dots: PbI_2 (96 mg, 0.21 mmol), ZnI_2 (67 mg, 0.21 mmol), 0.62 mL erucic acid, 83 μL R/S-MBA (or R/S-MBA carbon dots) and 667 μL oleylamine, and 5 mL ODE were mixed together into a 50 mL three-neck flask.

This mixture was heated at 120 °C for 45 minutes under nitrogen to dissolve the metal precursors. Afterward, the temperature was set up as 80 °C, followed by a rapid injection of 0.5 mL cesium oleate solution. After 5 seconds, the flask was immediately immersed in a water bath to quench the reaction. The solution was centrifuged at 3500 rpm for 7 minutes, the supernatant was decanted, and the centrifuged solid was dispersed in toluene for further characterizations and assembly experiments.

Assembly experiment: 30 μL of the $CsPbI_3$ nanoplatelets toluene solution (20 mg/mL) was drop-cast onto a glass slide by pipette. After several minutes of evaporation, the assembled nanoplatelets film was obtained (Figure S3).

Structure Characterizations

X-ray diffraction (XRD) test. The Miniflex 600 benchtop X-ray diffractometer was employed to test XRD patterns. This XRD diffractometer is equipped with a 0.6 kW Cu Kα X-ray tube and a HyPix-MF two-dimensional area detector, operating at a voltage of 45 kV and a current of 15 mA. During the measurement process, several drops of the nanoplatelets solution were applied onto a clean silicon substrate using a pipette. After solvent evaporation, XRD pattern scanning was performed. The scanning angle range was set from 5° to 80°, with a scanning rate of 10°/min.

Small-angle X-ray scattering (SAXS) test. SAXS data were recorded using the Xenocs Xeuss 3.0 instrument, with a q-range of 0.013 - 0.78 $Å^{-1}$.

Optical Microscope (OM) test. OM images were acquired using the SOPTOP RX50M microscope.

Scanning Electron Microscope (SEM) test. SEM images of the sample were acquired using a ZEISS Gemini 300 scanning electron microscope. To enhance the sample's conductivity, the glass slide was replaced by a silicon wafer.

Transmission Electron Microscope (TEM) test: The Tecnai G2 F20 S-TWIN TMP was used to record transmission electron microscopy (TEM) images at an operating voltage of 200 kilovolts. First, a carbon-coated copper mesh is placed on a silicon wafer. A drop of nanoplate-toluene suspension is then applied to the copper mesh and allowed to evaporate, forming a superlattice. To reduce sample concentration, the same procedure is performed, but the copper mesh is placed on lint-free paper instead. After solvent evaporation, monodisperse nanoplates are formed.

Optical property characterization

UV-Vis absorption test. The absorption spectra of the nanoplatelets solution were measured using a Shimadzu UV-2600i ultraviolet-visible spectrophotometer. The starting wavelength of the test is 300 nm, and the ending wavelength is 800 nm.

Photoluminescence (PL) and Variable-temperature fluorescence spectroscopy tests. The fluorescence spectra of the nanosheet solution were measured on a SHIMADZU RF-6000. The temperature-programmed fluorescence spectra were measured on an EDINBURGH FLS-1000. The variable temperature test was conducted from 30 K to 290 K, with one fluorescence spectrum collected every 20 K.

Circular Dichroism (CD) test. CD spectra were recorded on Chirascan V100 spectrophotometer, CD spectra were collected using a four-scan method[2]. Specifically, the thin-film sample was fixed on the test stage, which was rotated to four angles (0°, 90°, -0°,

and -90°). The average of the four collected CD signals was calculated as the sample's "pure" CD signal.

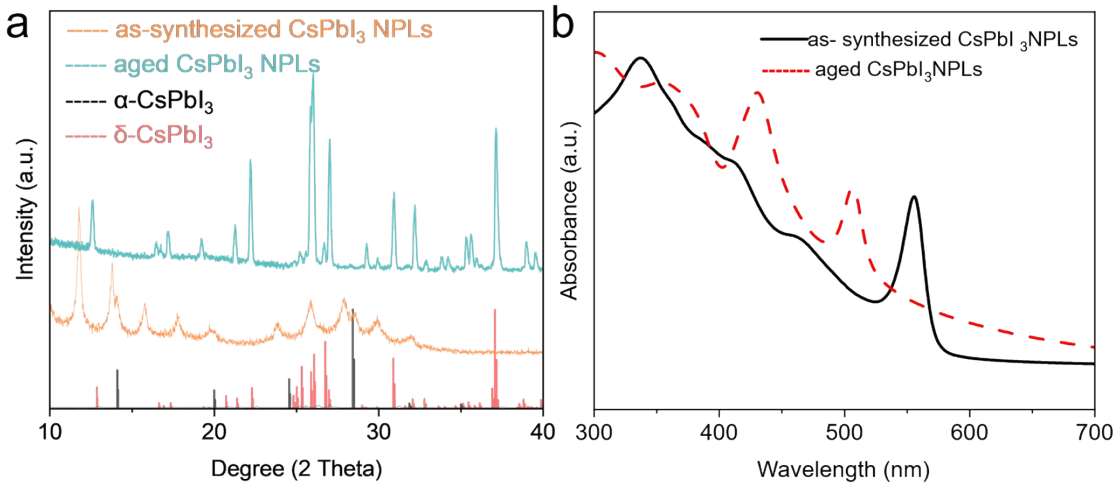

Figure S1: XRD patterns (a) and absorption spectra (b) of as-synthesized and aged $CsPbI_3$ NPLs.

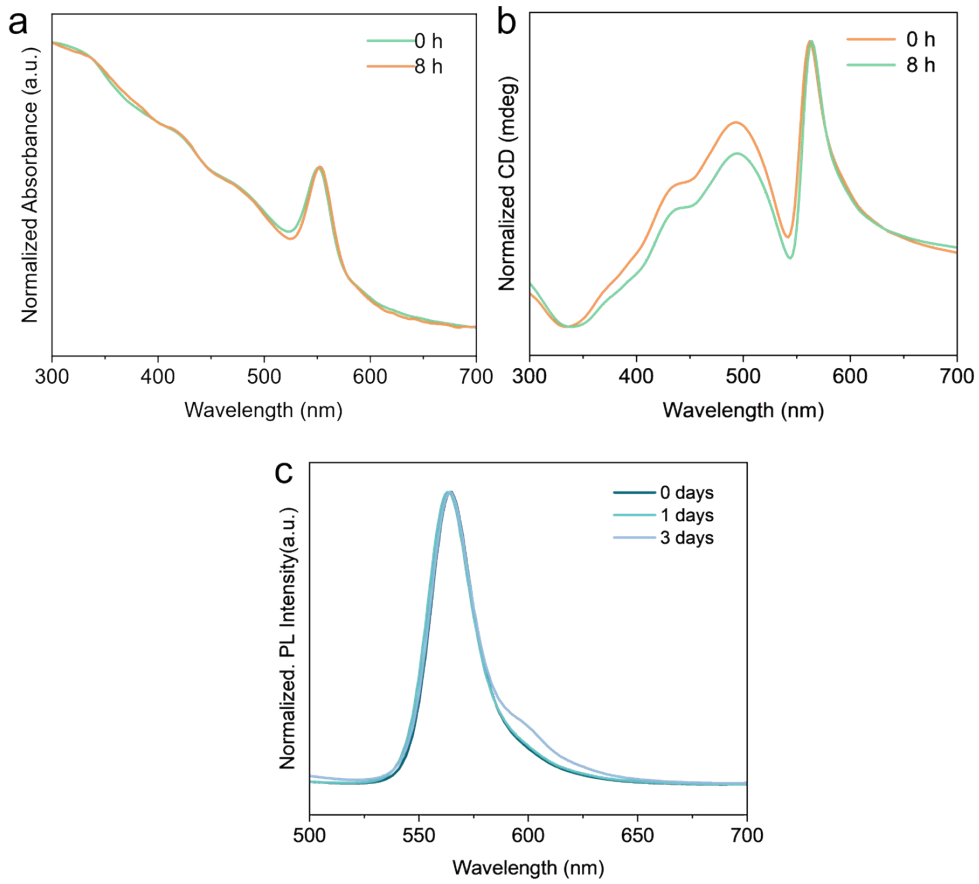

Figure S2: Absorption (a) and CD spectra (b) of the initial superlattice film and after being placed for 8 hours. (c) PL spectra of the fresh NPLs solution and the NPLs solution placed for 3 days.

Element	Sample content (mg/L)	Molar ratio
Cs	1.3435	0.904
Pb	2.3170	1
Zn	0.0105	0.0144

Table S1: ICP-OES result of 2 ML CsPbI3 NPLs.

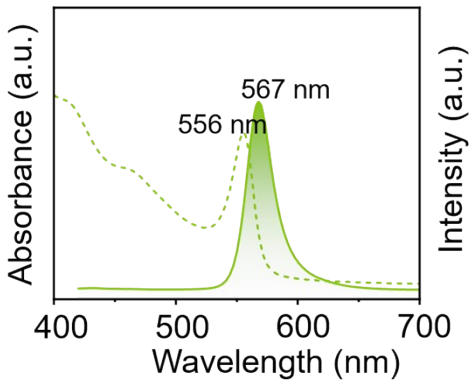

Figure S3: The band absorption and emission of $CsPbI_3$ nanoplatelets.

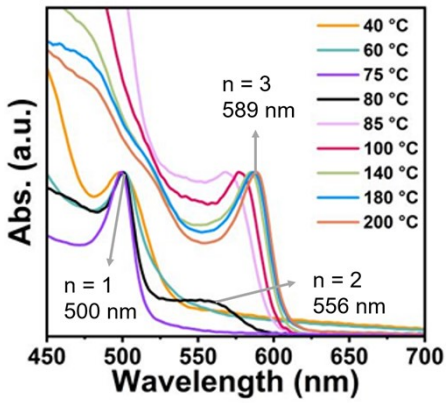

Figure S4: The band absorption of $CsPbI_3$ nanoplatelets with different monolayer thicknesses (n=1, 2, 3).[40]

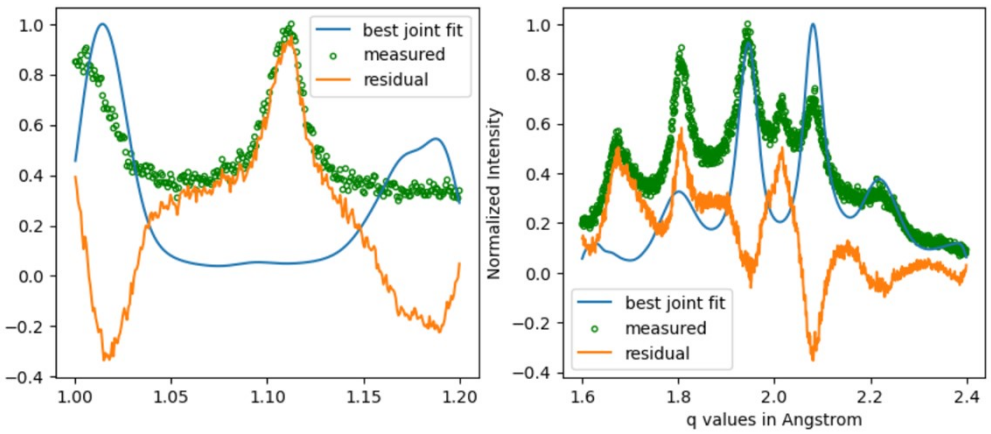

Figure S5: XRD peak fitting results followed by an open-source fitting algorithm developed by Toso et. Al[3].

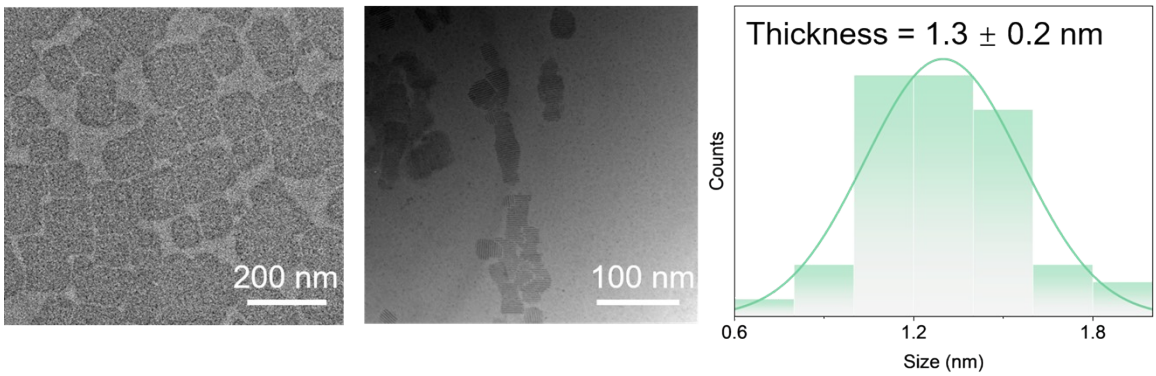

Figure S6: TEM image of nanoplatelets stacked face-down and along the thickness direction. Statistical graph of the thickness of 50 nanoplatelets.

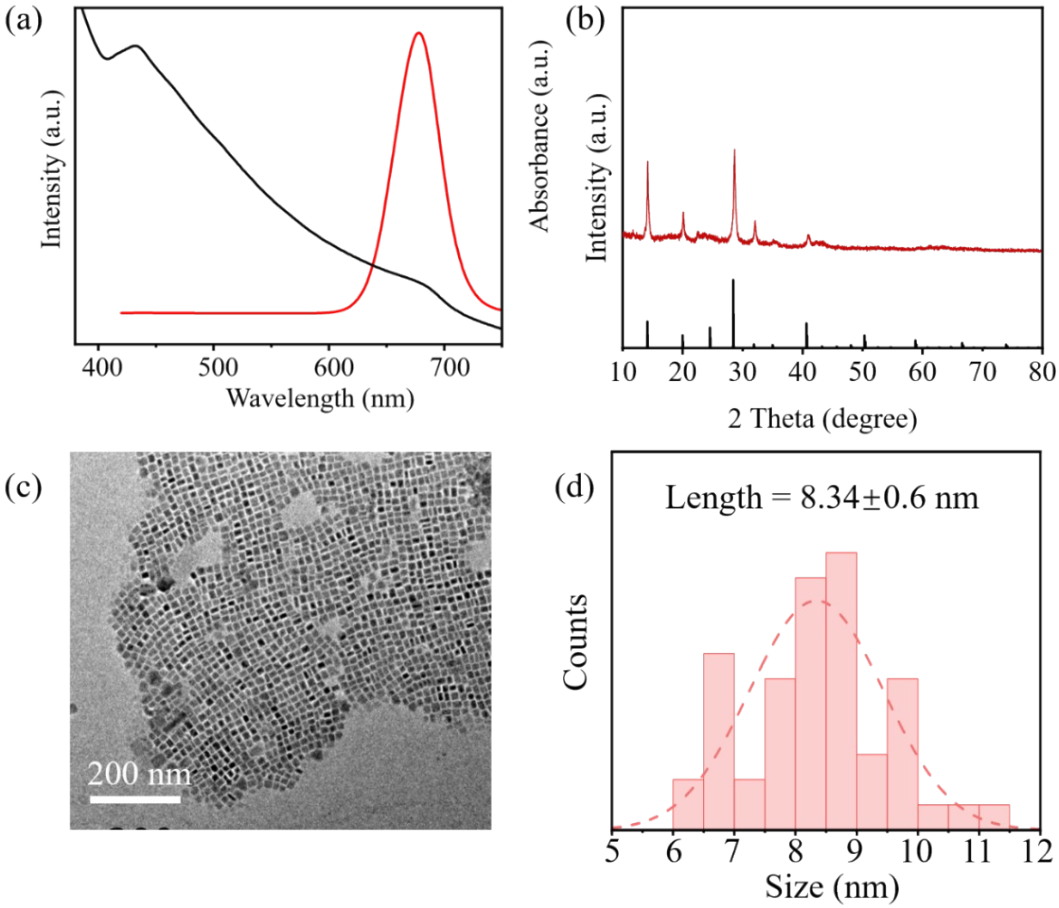

Figure S7: (a) UV-visible absorption spectrum and fluorescence spectrum of $CsPbI_3$ nanocrystals. (b) XRD diffraction pattern of $CsPbI_3$ nanocrystals. (c) TEM image of $CsPbI_3$ nanocrystals. (d) Particle size distribution diagram of $CsPbI_3$ nanocrystals.

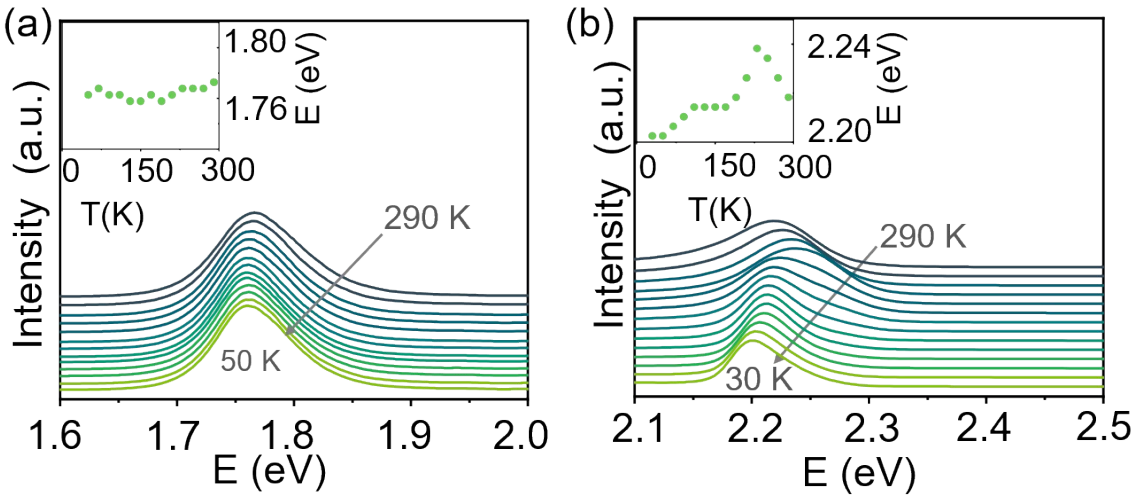

Figure S8: (a) Temperature dependent photoluminescence of $CsPbI_3$ nanocrystals (d = 8.3 nm). (b) Temperature dependent photoluminescence of 2 ML $CsPbI_3$ nanoplatelets.

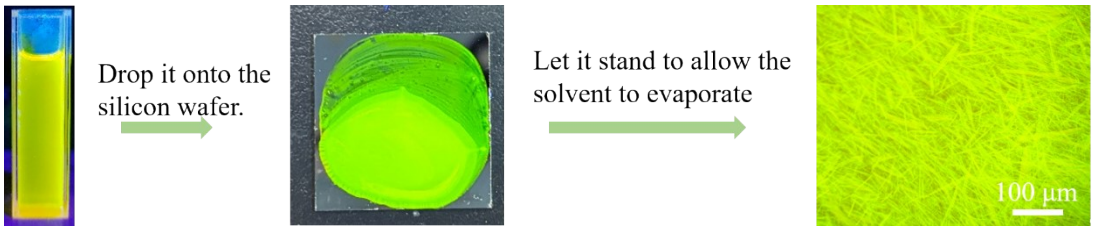

Figure S9: Photos of the assembly process. Place the silicon wafer on the desktop. Take 30 microliters of NPLs solution (20 mg/ml), drop it onto the silicon wafer, and keep it still until the solvent evaporates completely.

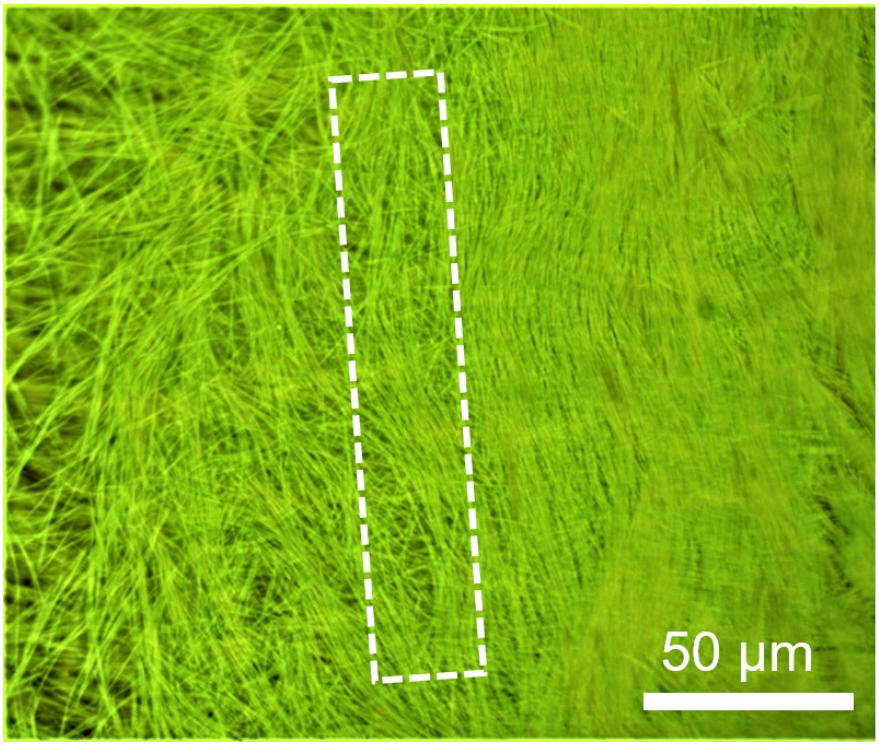

Figure S10: Optical microscope one-dimensional superlattices. The dashed rectangular shapes mark the direction of one-dimensional superlattices.

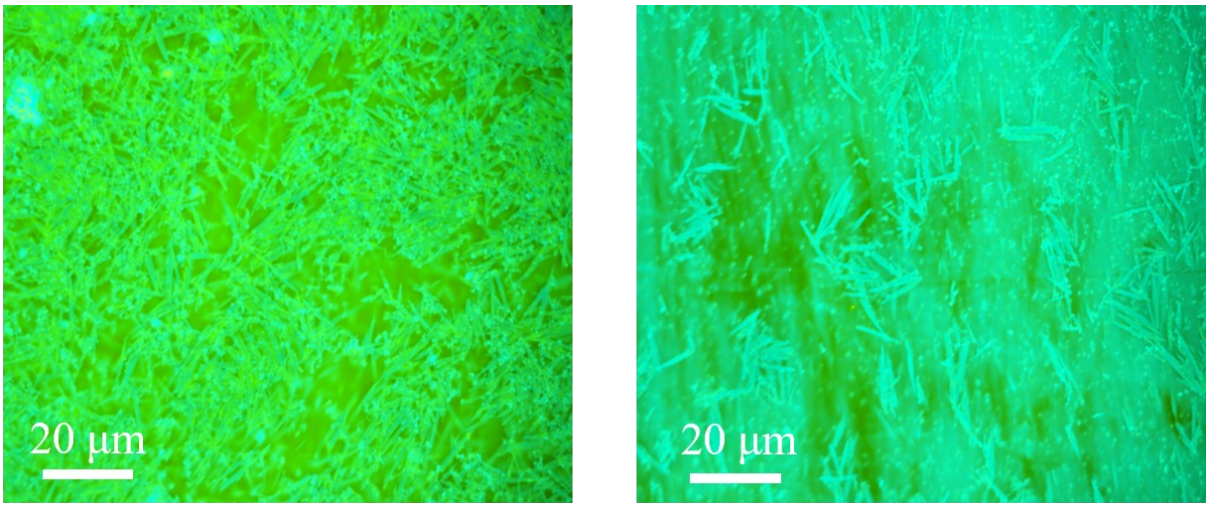

Figure S11: OM images of superlattices assembled by 2 ML $CsPbI_3$ nanoplatelets dispersed in heptane (left) and octane (right) solution, respectively.

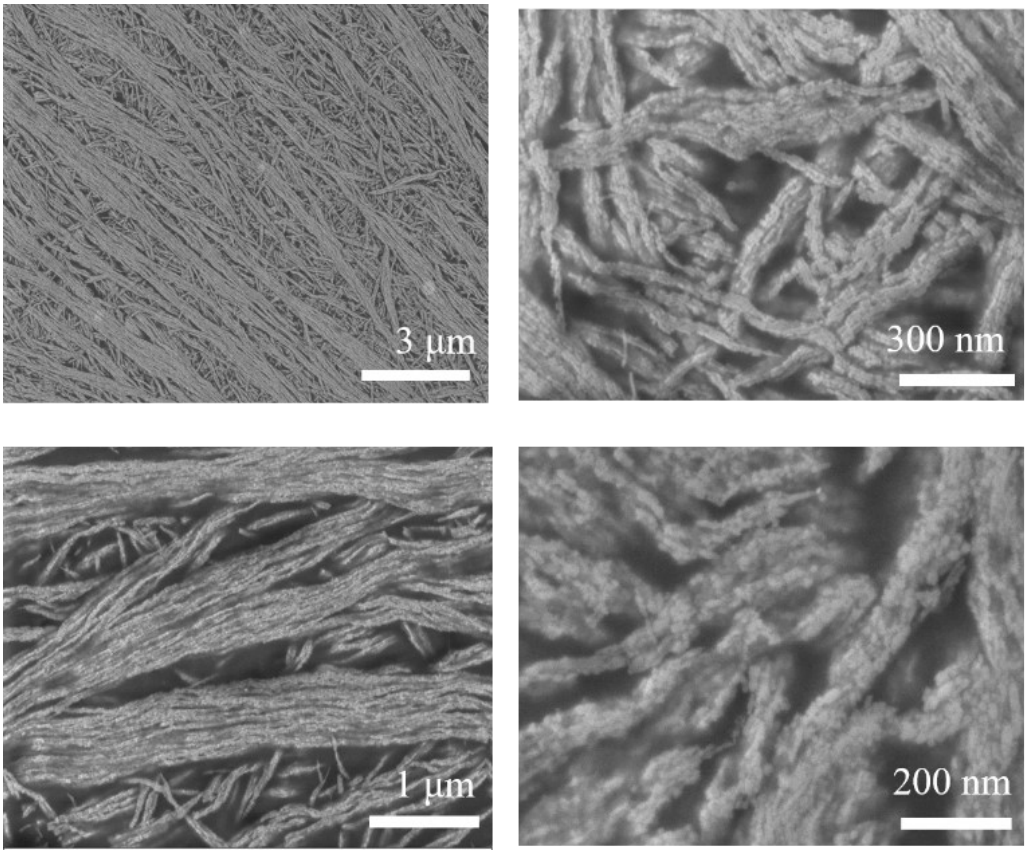

Figure S12: SEM images of 2 ML $CsPbI_3$ NPLs superlattices at different scales.

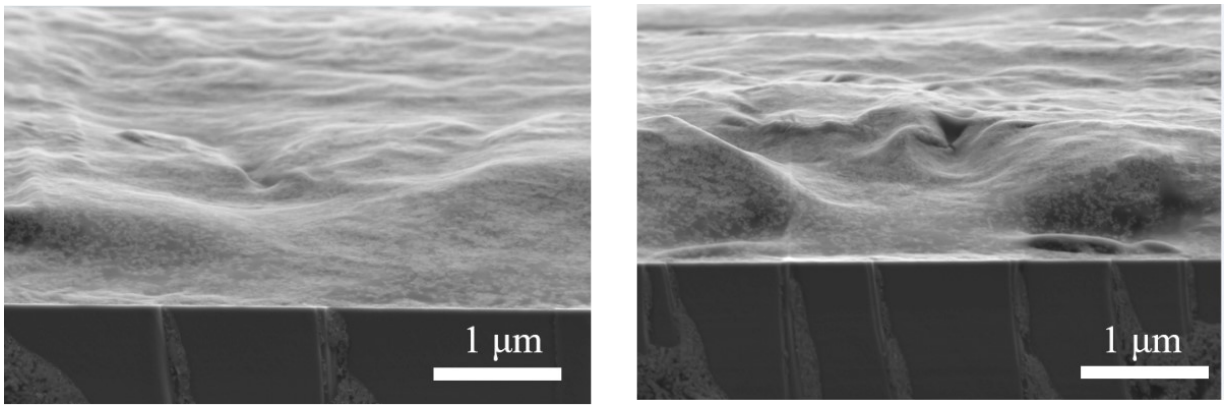

Figure S13: Cross-sectional SEM image of 2 ML $CsPbI_3$ NPLs superlattices.

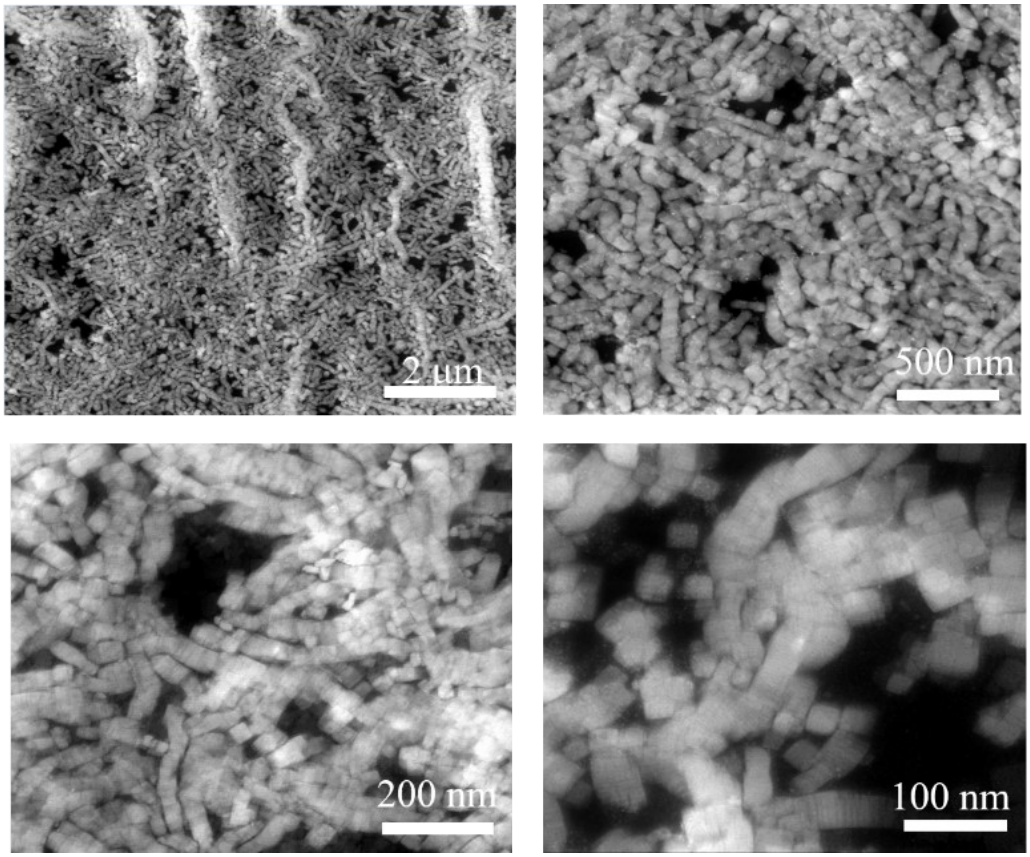

Figure S14: STEM images of 2 ML $CsPbI_3$ NPLs superlattices at different scales.

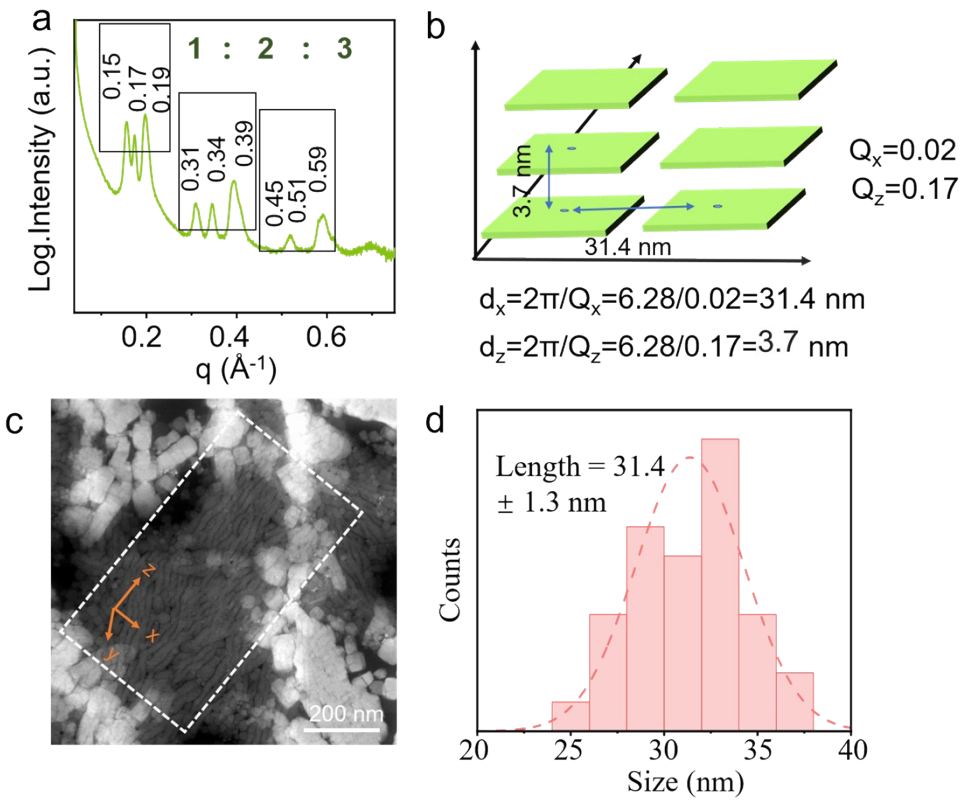

Figure S15: (a) Small angle X-ray scattering (SAXS) of 1D superlattices. (b) Schematic diagram of lamellar stacked nanoplatelets (right). STEM images of layered structures (c) and measurement of nanoplatelets length (d).

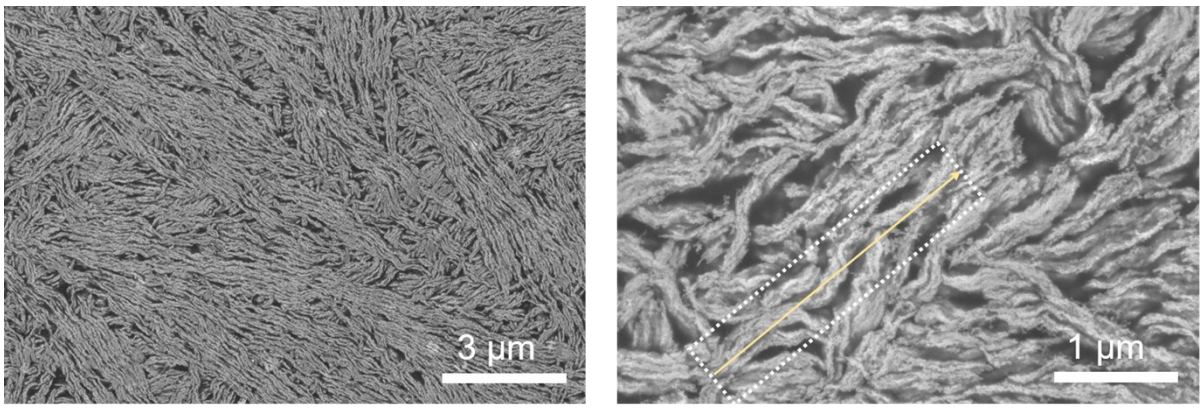

Figure S16: SEM images of one-dimensional spiral strips observed under different magnifications (a white box marks one of the spiral strips, and the internal arrow indicates the propagation direction of individual twists).

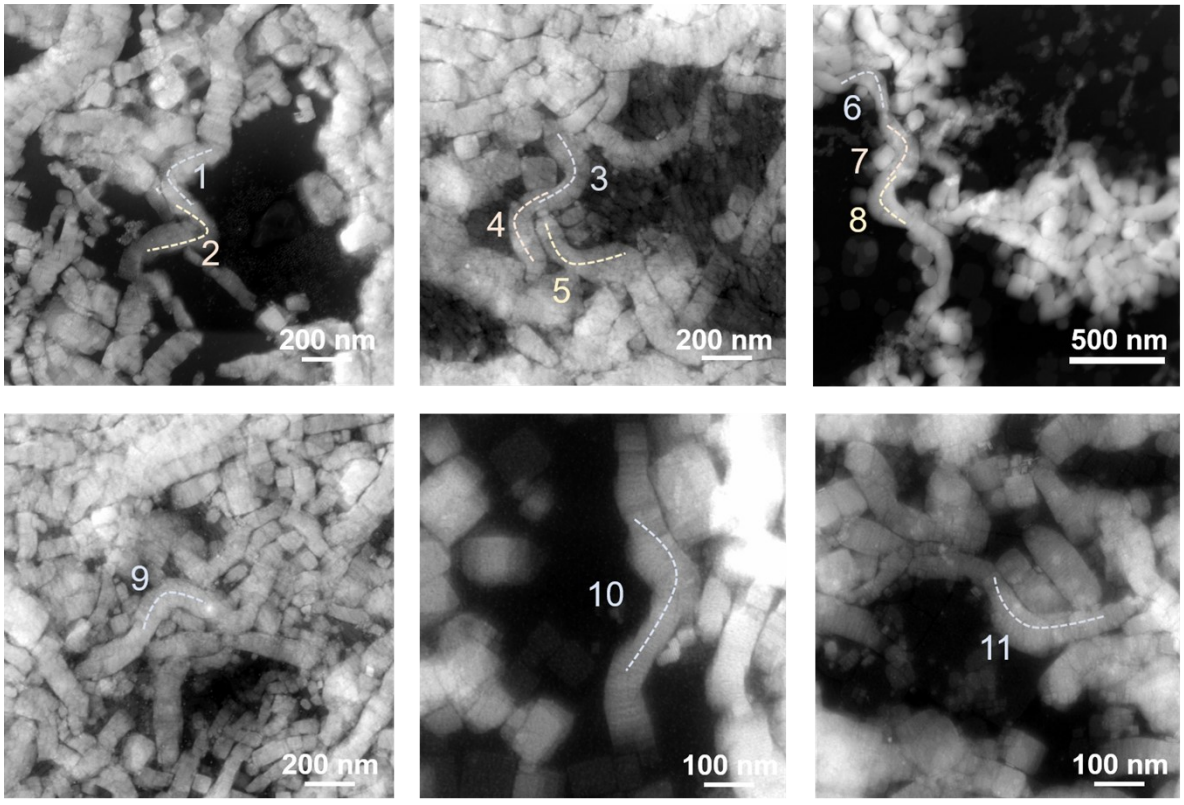

Figure S17: STEM image of one-dimensional helical superlattice (The dashed lines mark the measured helical structures in sequence).

Sample	Pitch (nm)	Diameter (nm)	Twist angle (°/nm)
1	318.7	350.93	1.13
2	271.54	410.62	1.33
3	171.92	226.65	2.09
4	185.06	240.22	1.95
5	274.70	195.95	1.31
6	298.98	446.36	1.20
7	298.98	348.44	1.20
8	348.44	378.86	1.03
9	261.8	183.83	1.38
10	252.78	201.6	1.42
11	256.88	341.17	1.40
Average	267.25	302.24	1.4

Table S2: Statistics of helical parameters of one-dimensional helical superlattice.

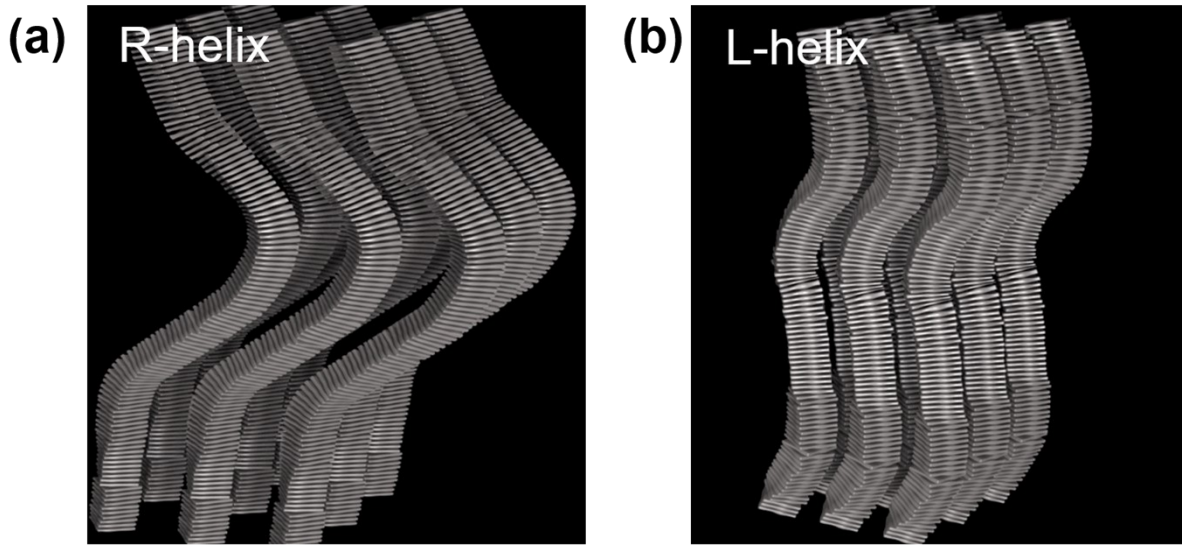

Figure S18: 3D model of (a) R-configured and (b) L-configured superlattices. The rotation angle of each NPL is calculated based on the width variation of NPL within nanoribbons in STEM (dashed green rectangles of Figure 3A-B). These models also consider the stacking of nanoribbons in the lateral direction (Figure 2E).

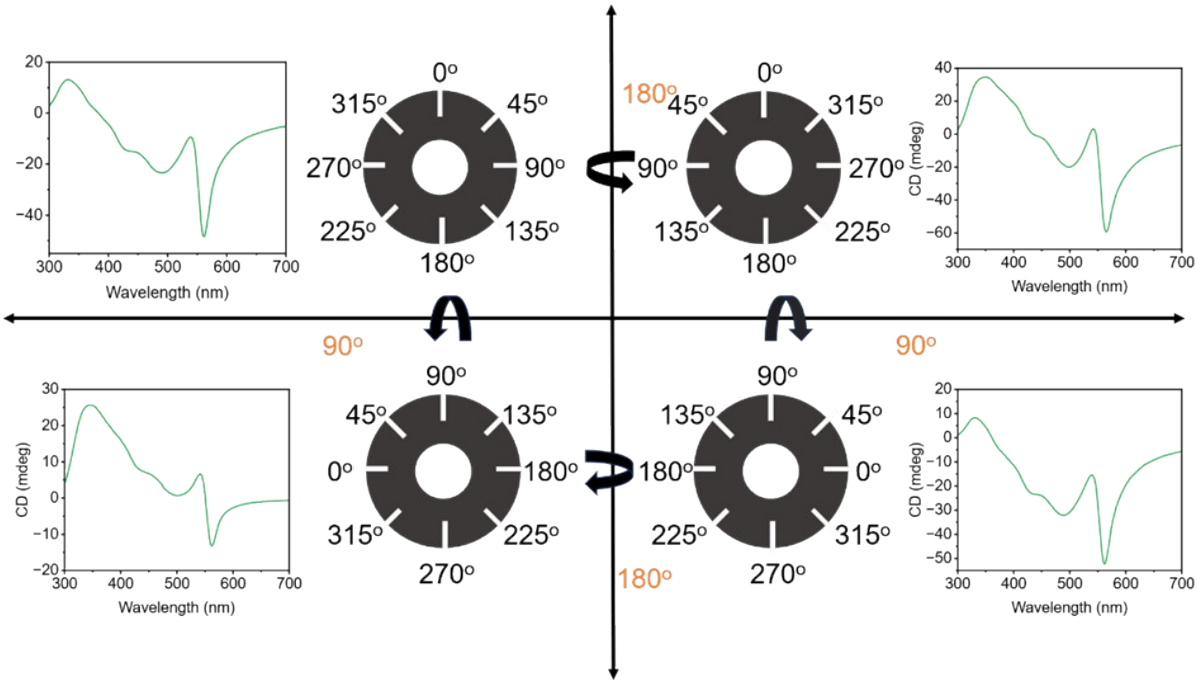

Figure S19: Schematic diagram of CD signal collection by four-scan method.

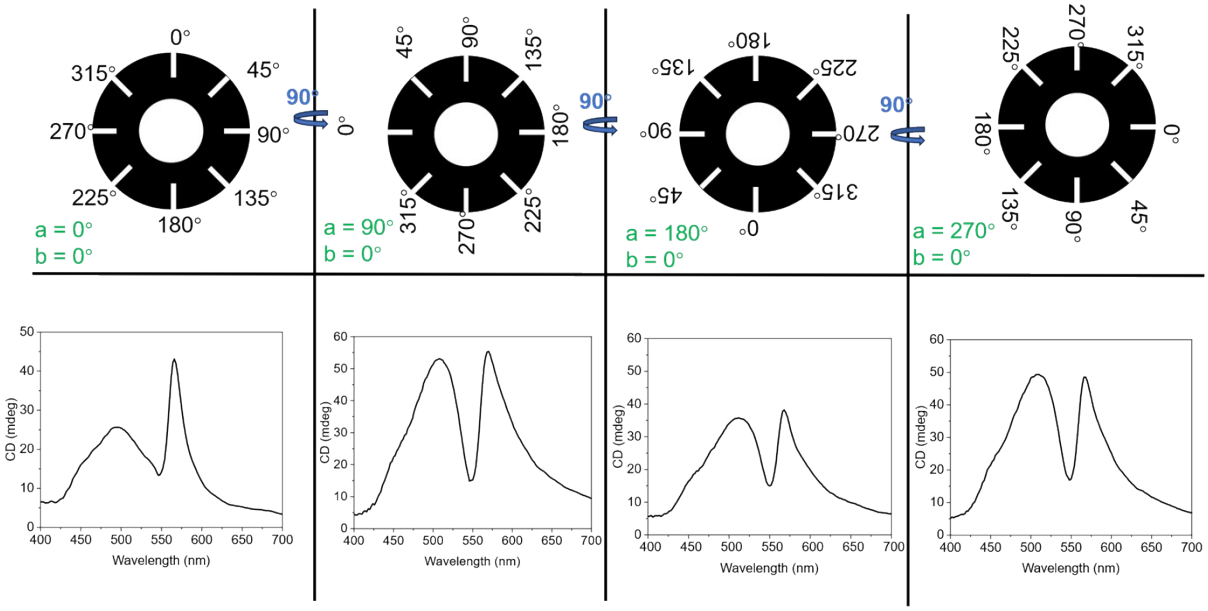

Figure S20: A schematic diagram of the standard method (rotating the sample to (0°, 0°), (90°, 0°), (180°, 0°), (270°, 0°) in one plane) for measuring circular dichroism signals.

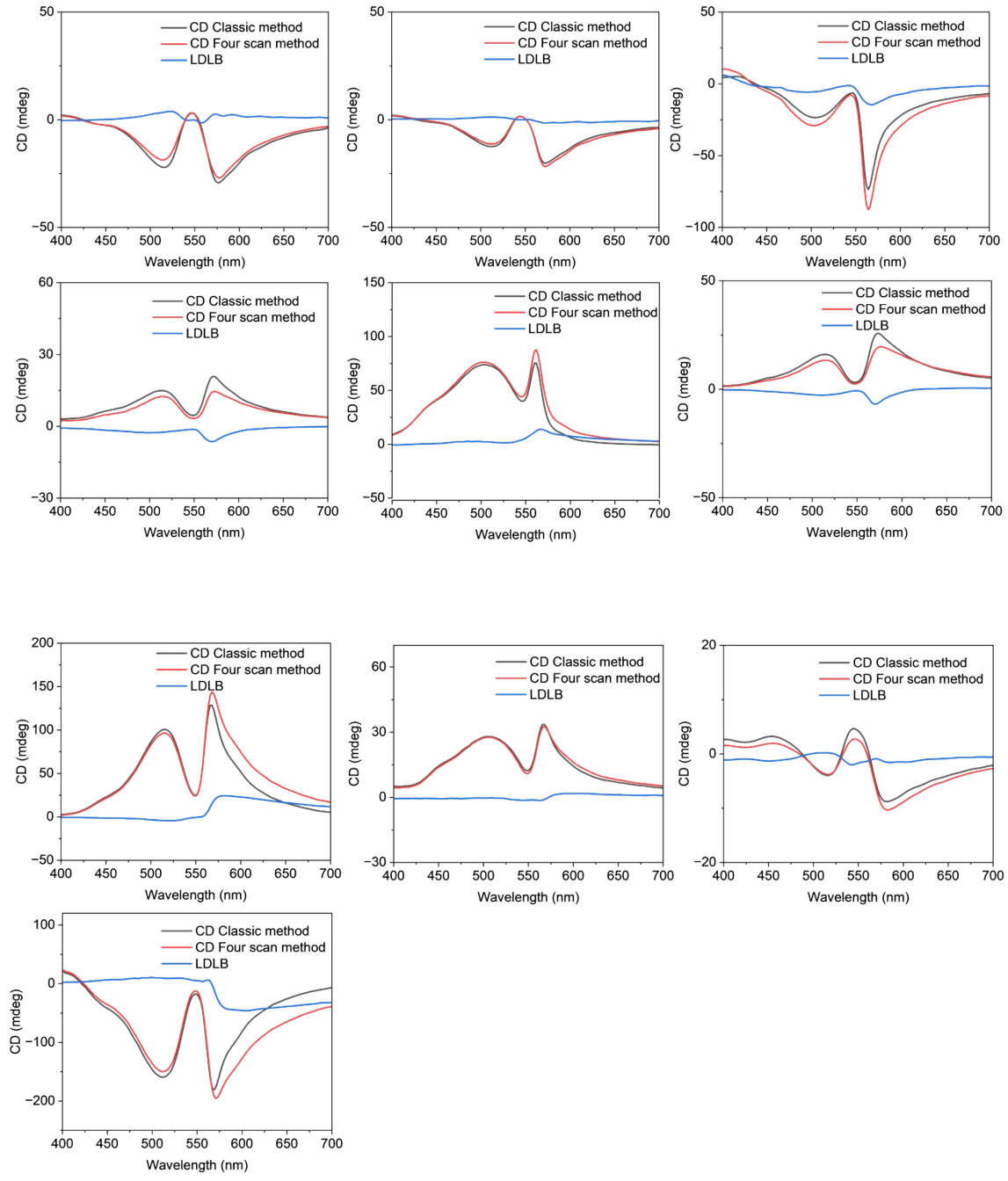

Figure S21: CD spectra obtained by 10 groups using the standard method and the four-scan method, respectively. The intensity difference is ascribed to LDLB effect.

Sample	$\int\|CD_{avg}\|$	$\int\|LDLB\|$	$\int\|LDLB\|/\int\|CD_{avg}\|$
1	87.64	12.24	0.14
2	87.63	14.02	0.16
3	143.88	15.39	0.11
4	194.65	15.16	0.11
5	68.23	2.99	0.08
6	28.80	2.59	0.09
7	21.17	1.09	0.05
8	25.68	6.23	0.24
9	33.62	1.01	0.03
10	10.23	1.63	0.16
11	41.64	6.08	0.15

Table S3: Statistical counting of the contribution of LDLB signals to CD signals. $\int|CD_{avg}|$ represents the observed CD signal by classical method, and $\int|LDLB|$ represents the LDLB intensity. $\int|LDLB|/\int|CD_{avg}|$ represents the contribution of LD in the observed CD signal.

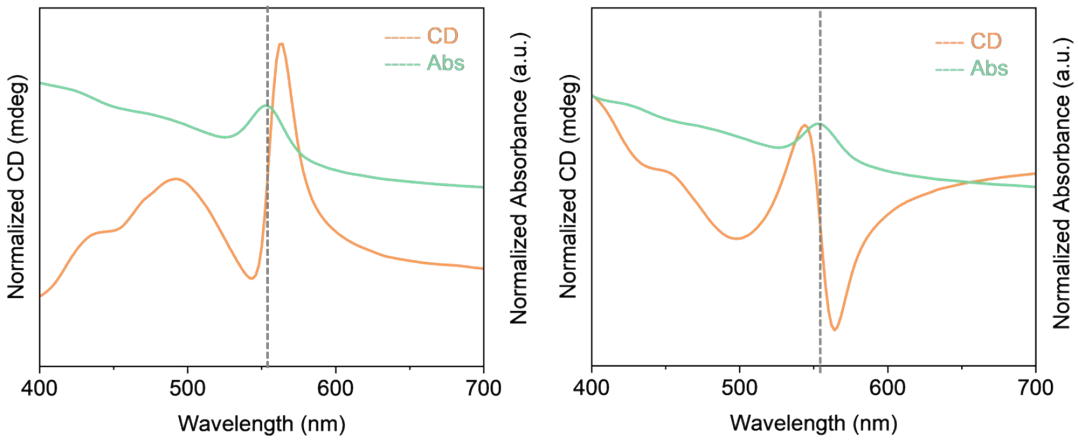

Figure S22: CD spectrum and ultraviolet absorption spectrum of one-dimensional superlattice thin films (the small box shows that the absorption exciton peak corresponds to the zero-crossing point of the alternating circular dichroism spectrum).

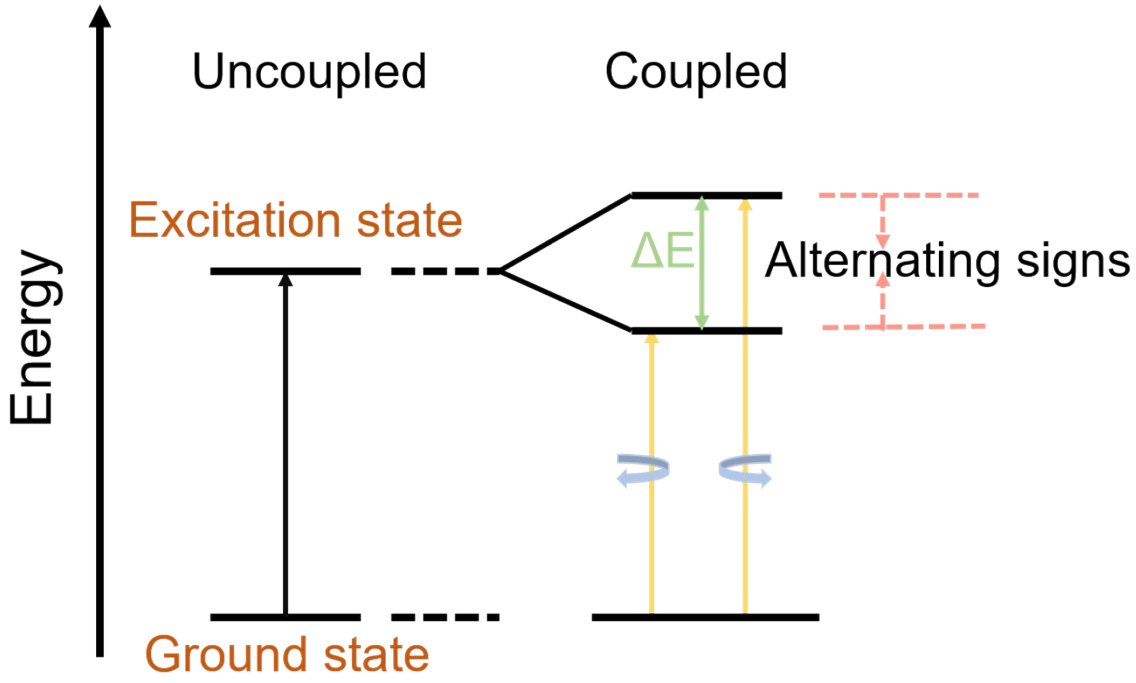

Figure S23: Schematic diagram of alternating circular dichroism signals caused by dipole-dipole interactions.

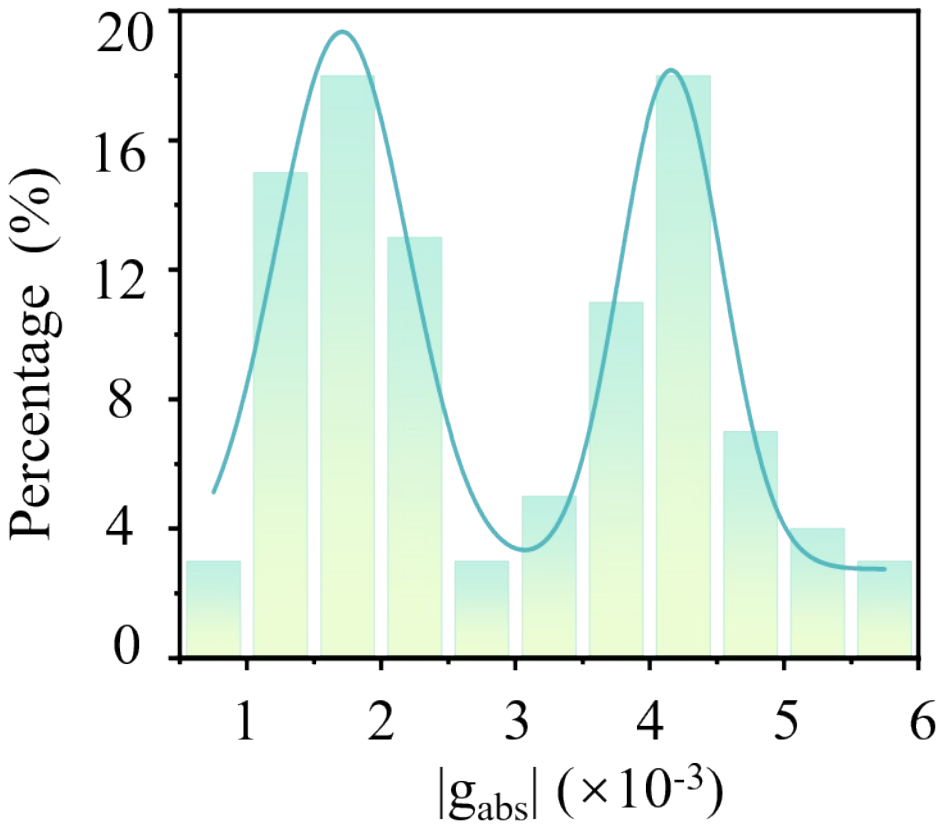

Figure S24: Distribution of anisotropy factor (g_{abs}) for 50 batches of NPLs superlattices.

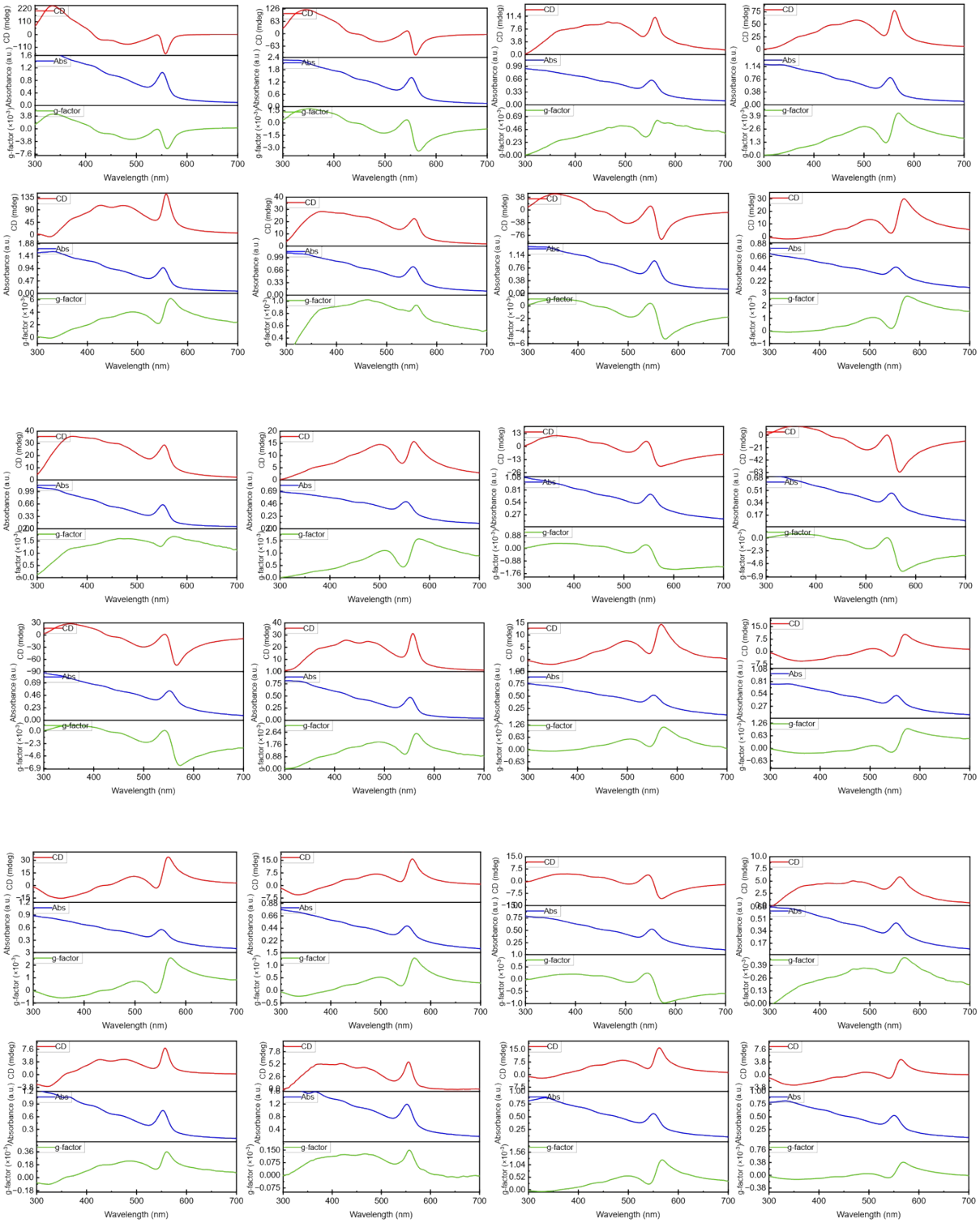

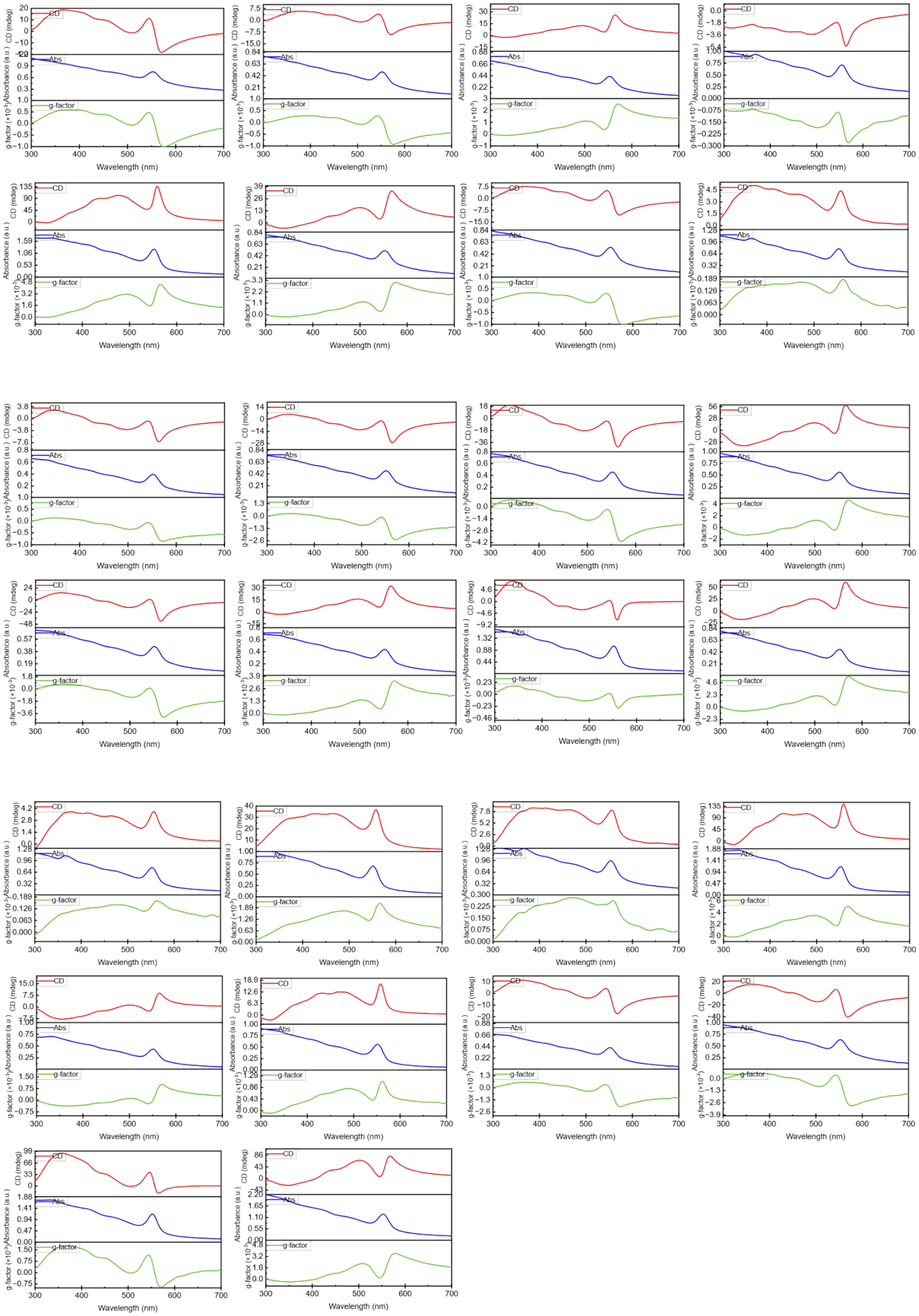

Figure S25: CD signals of 2 ML $CsPbI_3$ NPLs superlattices. (50 batches).

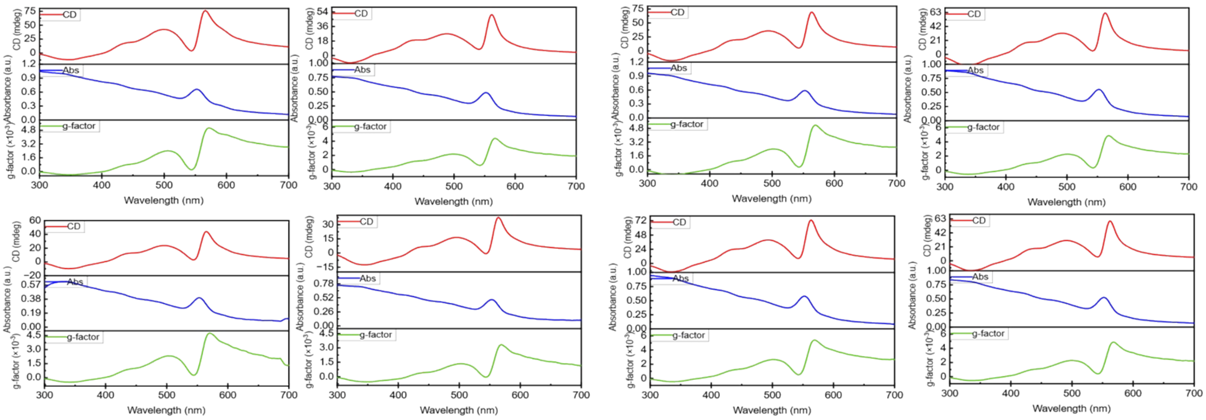
CD
Abs
g-factor
CD (mdeg)
Absorbance (a.u.)
g-factor (×10⁻³)
Wavelength (nm)

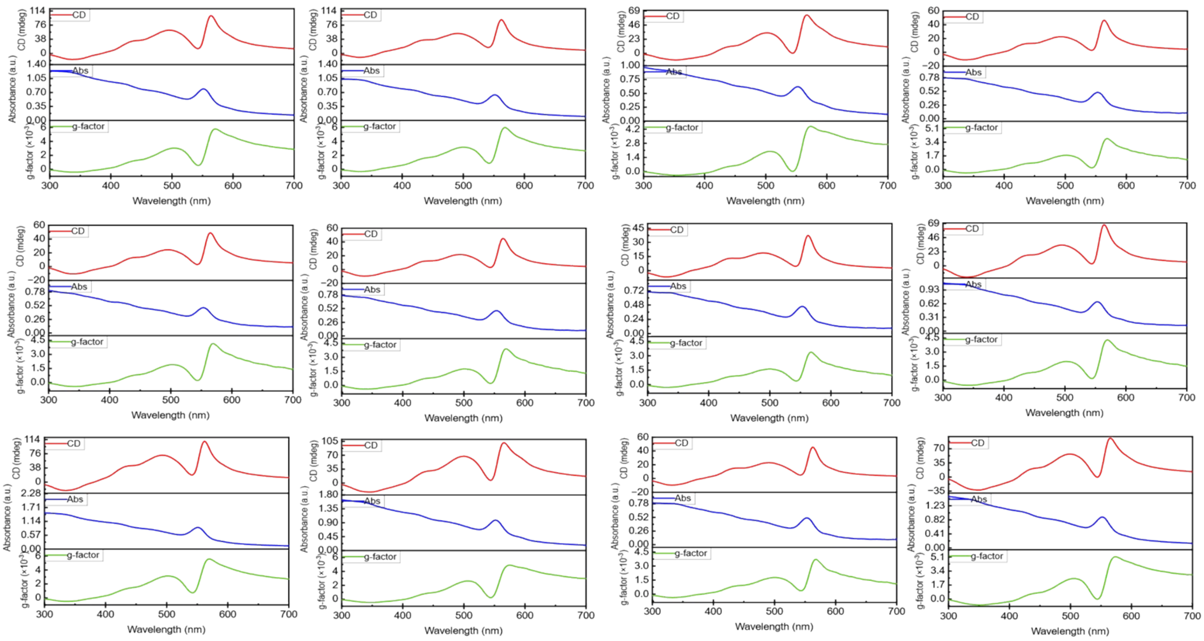
CD
Abs
g-factor
CD (mdeg)
Absorbance (a.u.)
g-factor (×10⁻³)
Wavelength (nm)

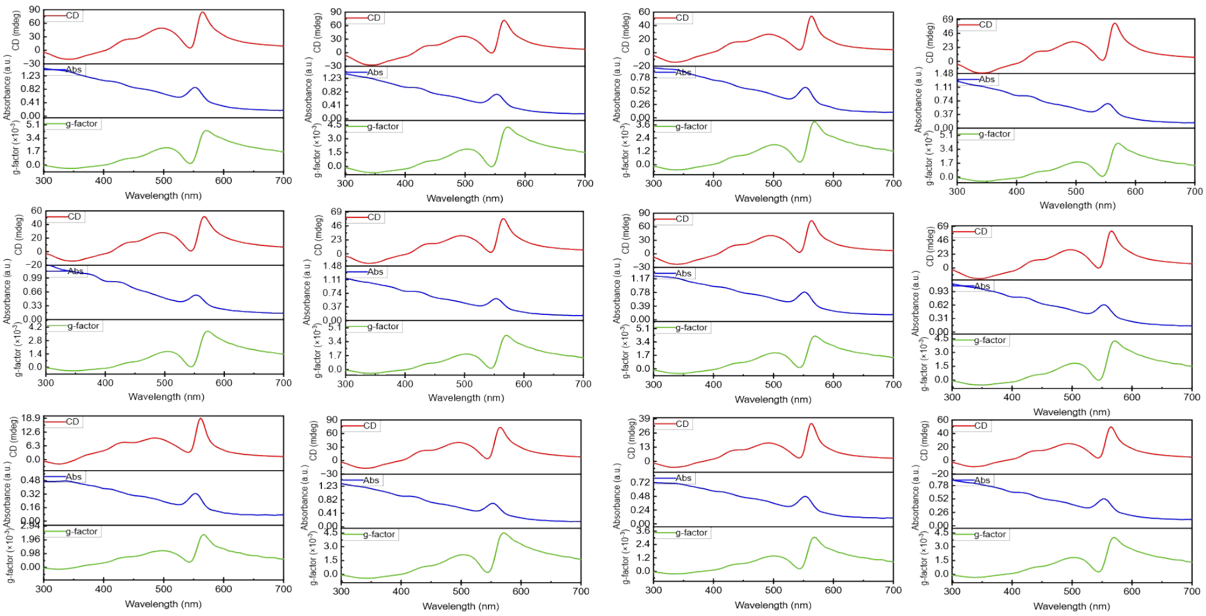
CD
Abs
g-factor
CD (mdeg)
Absorbance (a.u.)
g-factor (×10⁻³)
Wavelength (nm)

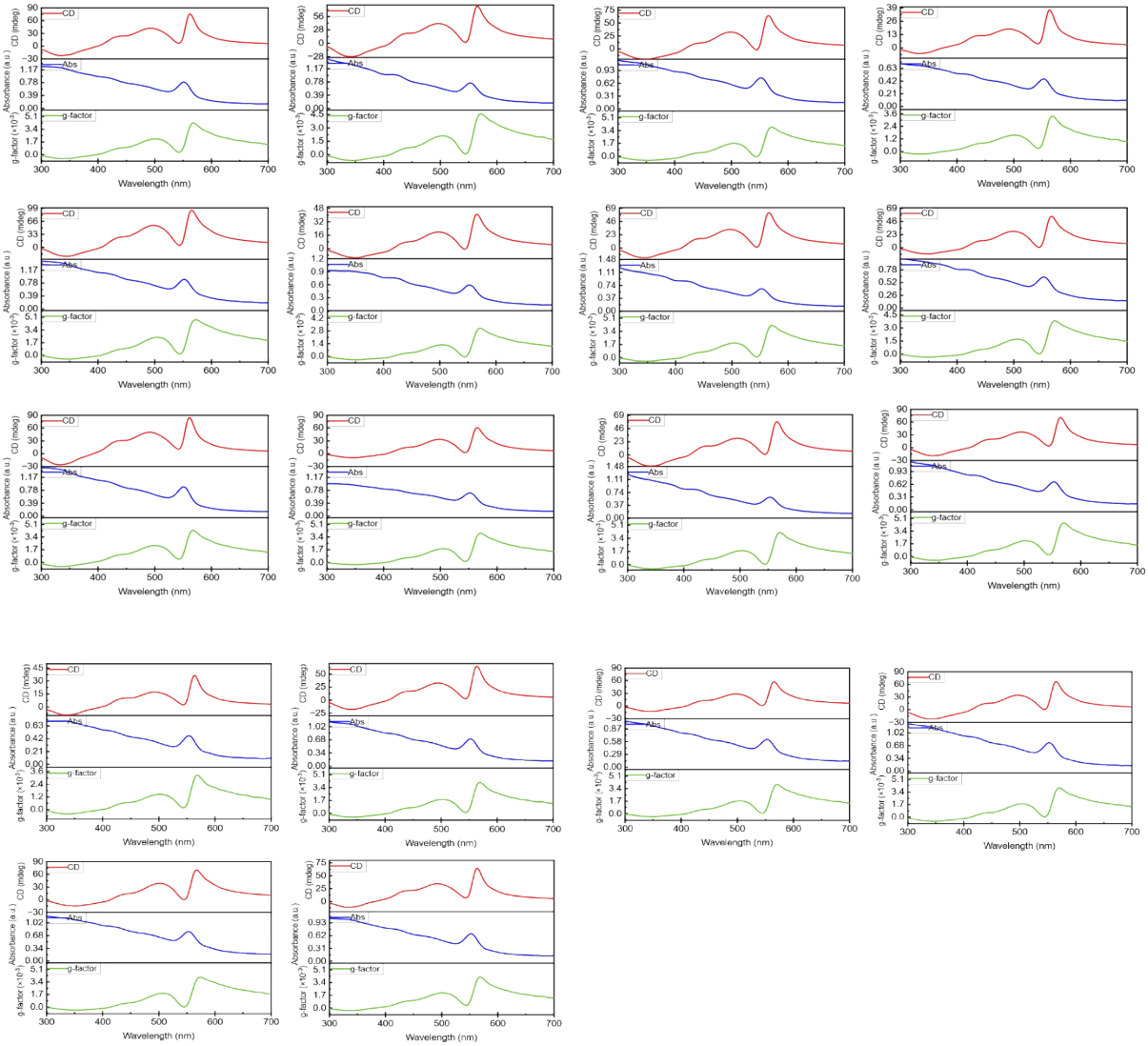

Figure S26: CD signals of 2 ML $CsPbI_3$ NPLs superlattices after adding R-MBA ligands (50 batches).

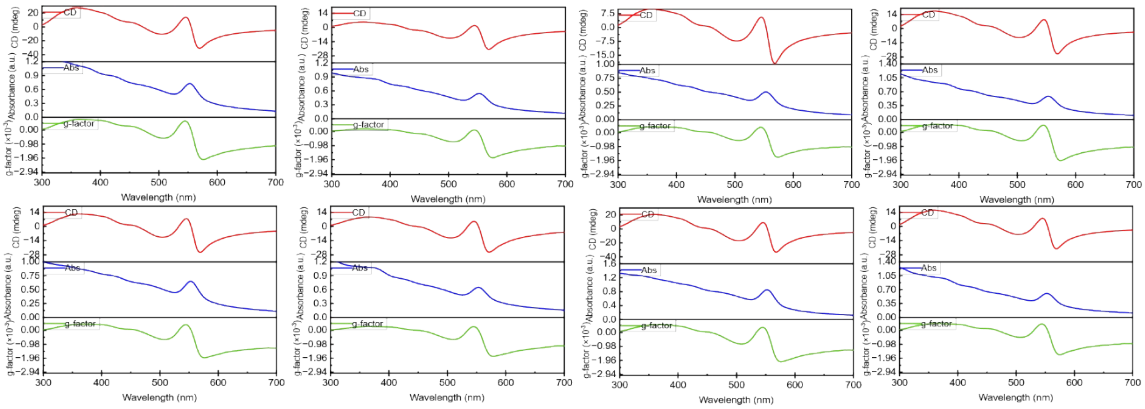

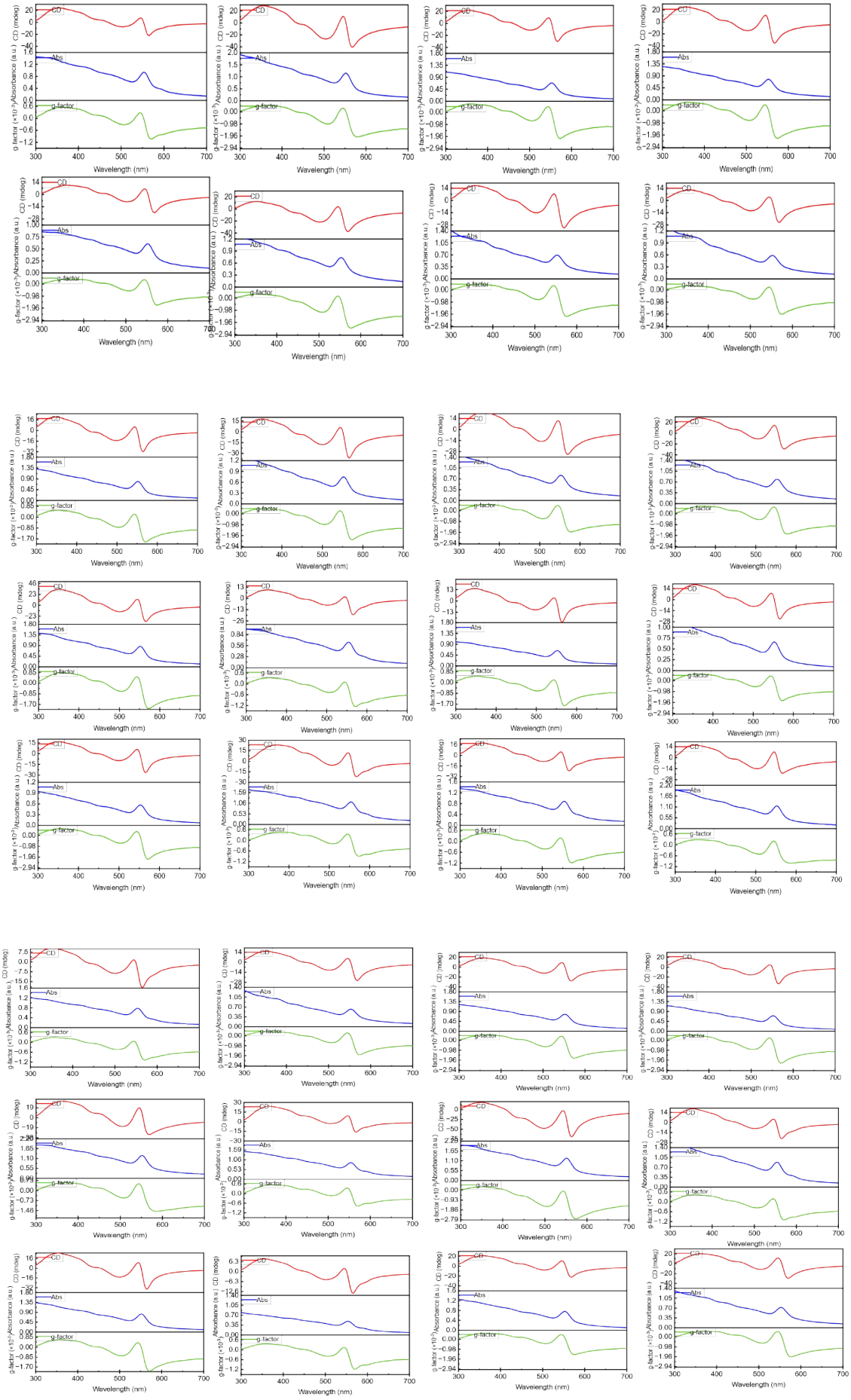
CD
Abs
g-factor
Wavelength (nm)

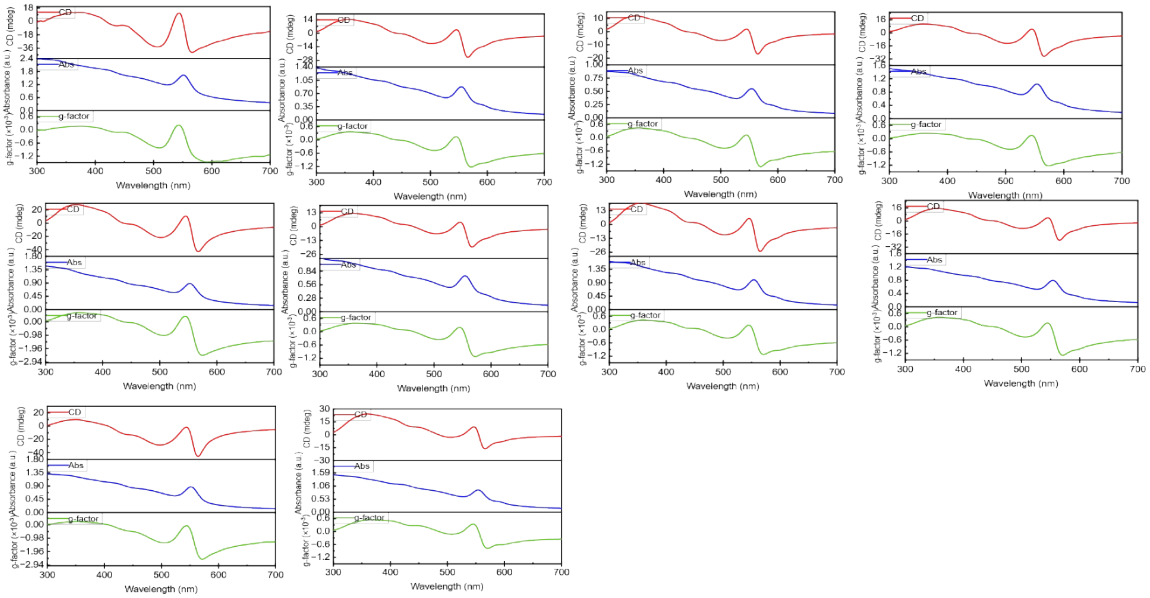

Figure S27: CD signals of 2 ML $CsPbI_3$ NPLs superlattices after adding S-MBA ligands (50 groups).

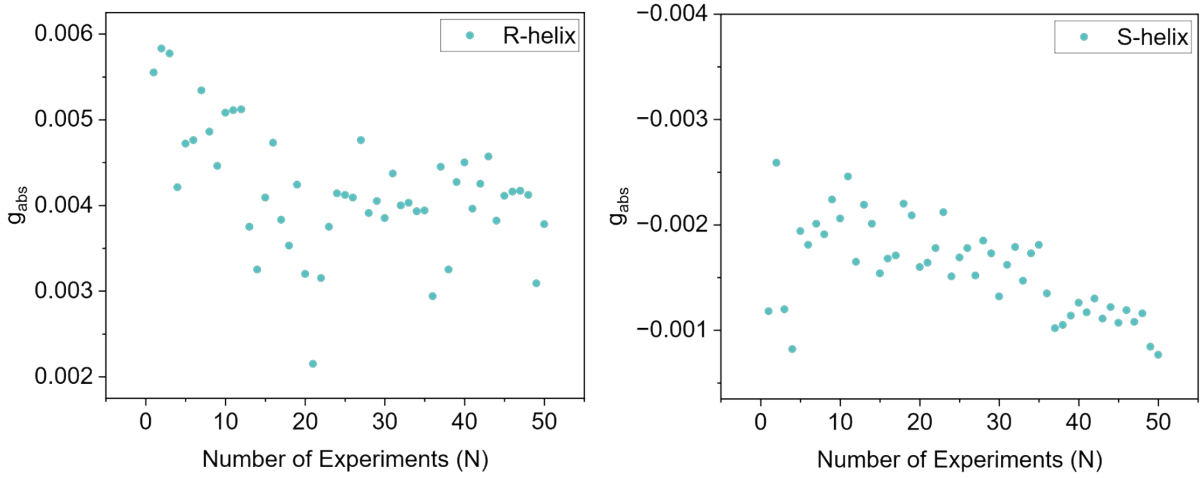

Figure S28: The g_{abs} values (50-batches) after R/S-MBA treatment.

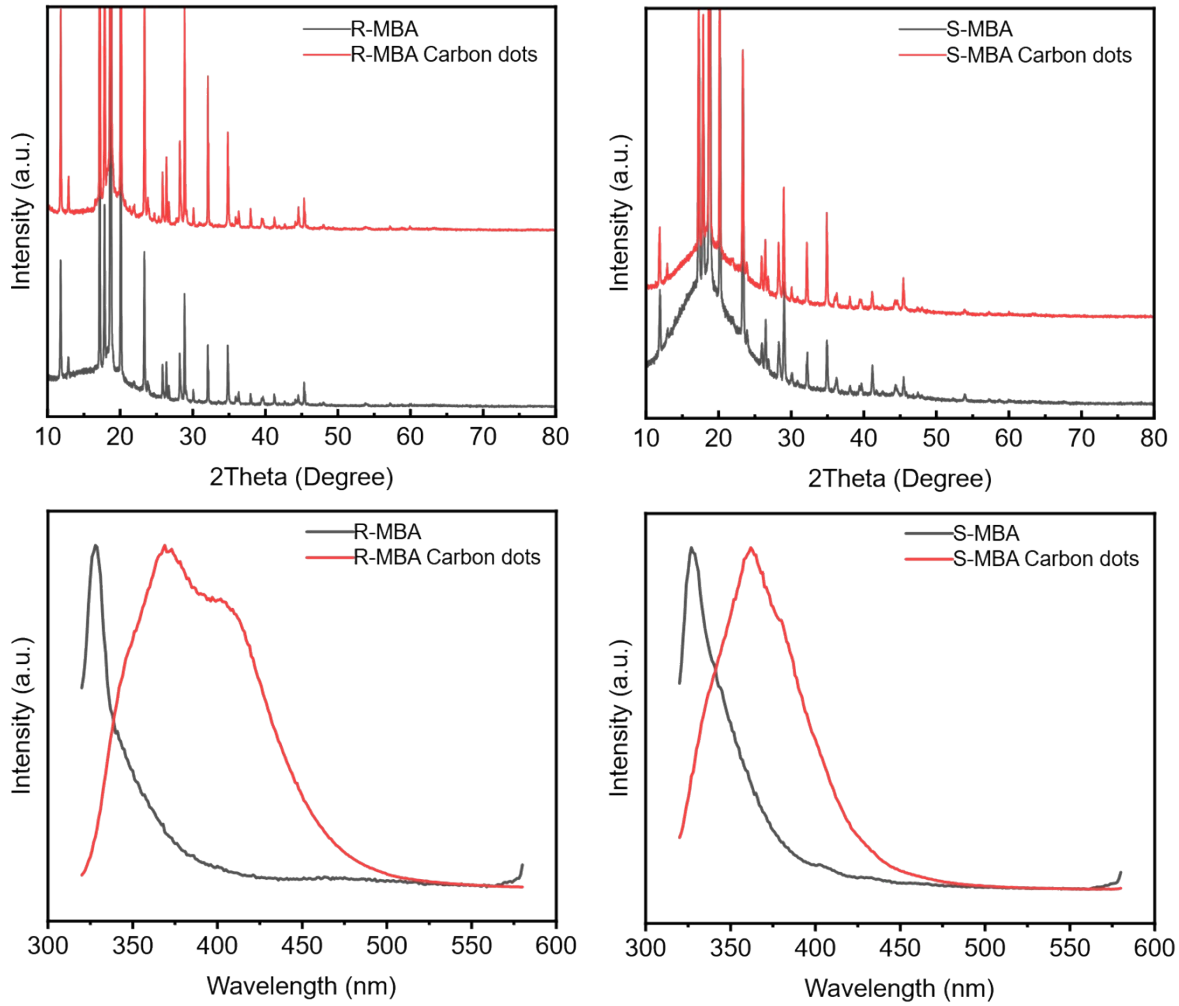

Figure S29: XRD and fluorescence spectrum of R/S-MBA and R/S-MBA carbon dots.

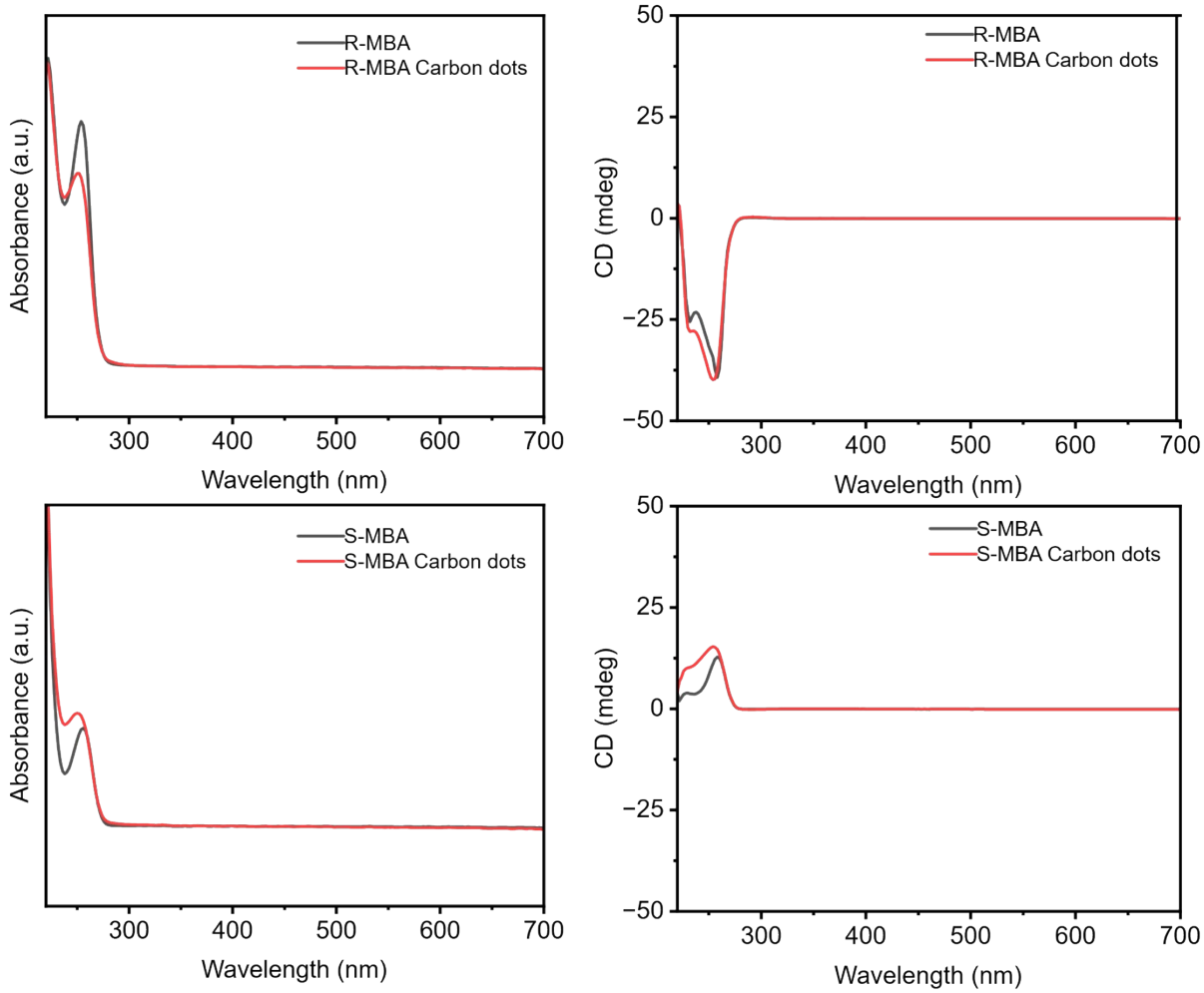

Figure S30: UV-visible absorption spectrum and CD signals of R/S-MBA and R/S-MBA carbon dots.

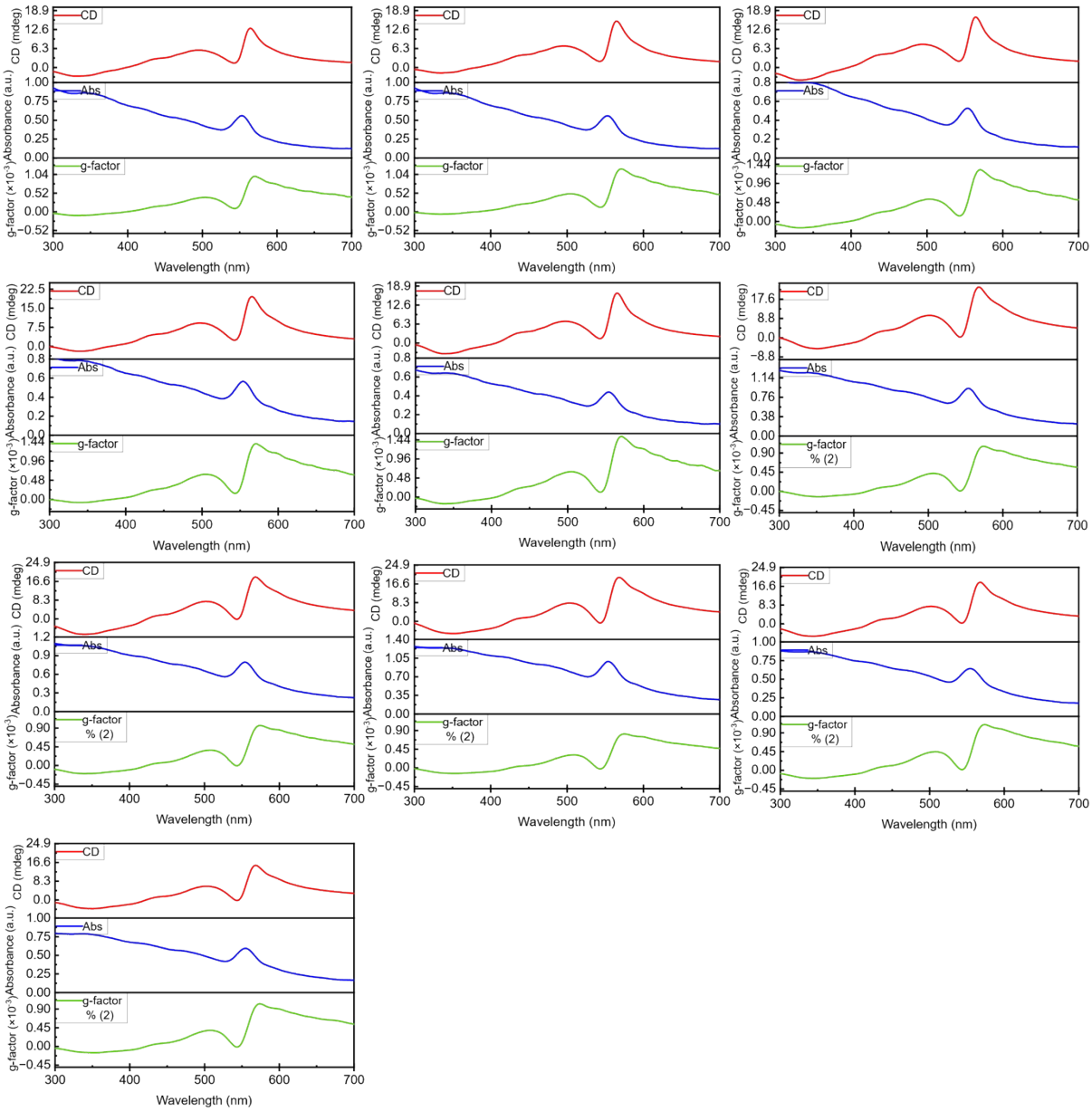

Figure S31: CD signals of 2 ML $CsPbI_3$ NPLs superlattices after adding R-MBA carbon dots (10 batches).

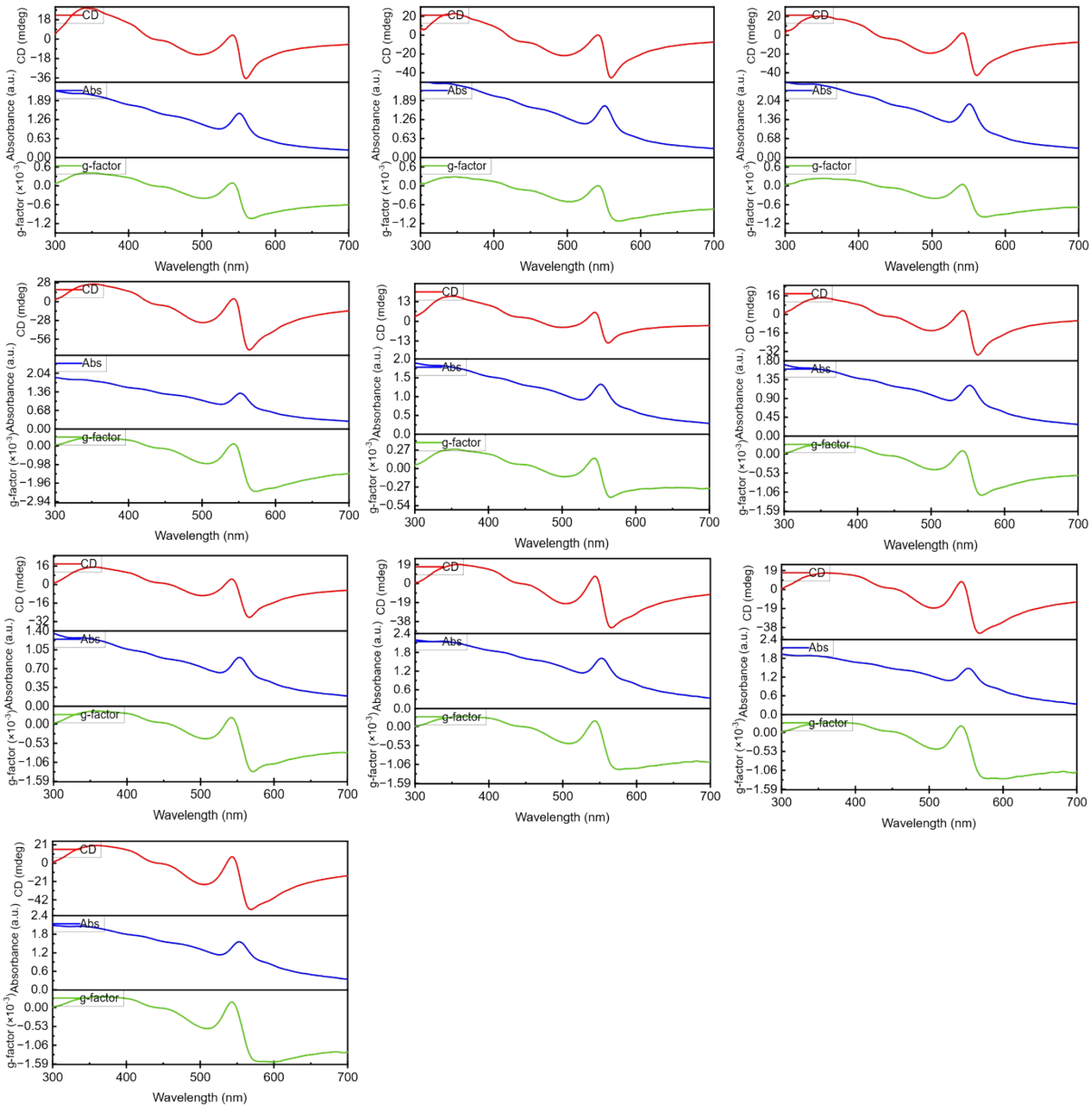

Figure S32: CD signals of 2 ML $CsPbI_3$ NPLs superlattices after adding S-MBA carbon dots (10 batches).

References:

(1). Q. A. Akkerman, D. Meggiolaro, Z. Dang, F. De Angelis, L. Manna, Fluorescent Alloy $CsPb_xMn_{1-x}I_3$ Perovskite Nanocrystals with High Structural and Optical Stability. *ACS Energy Letters* 2, 2183-2186 (2017).

(2). Y. Yao *et al.*, Extracting Pure Circular Dichroism from Hierarchically Structured CdS Magic Cluster Films. *ACS Nano* **16**, 20457-20469 (2022).

(3). S. Toso, D. Baranov, D. Altamura, F. Scattarella, J. Dahl, X. Wang, S. Marras, A. P. Alivisatos, A. Singer, C. Giannini, L. Manna, *ACS Nano* **2021**, *15*, 6243-6256.